

Performance of the WFC3-IR channel with FPA#64

M. Stiavelli and M. Robberto
May 12, 2003

Abstract

We document the model used to assess the performance of the IR channel of WFC3 with FPA#64. We show that the WFC3 IR channel meets the high-level CEI spec sensitivity requirements and exceeds the performance described in the more detailed low-level CEI specs. We define a discovery efficiency metric and show that the instrument exceeds the discovery efficiency of post-NCS NICMOS by a factor 10 and that of the pre-NCS NICMOS by a factor 15.

1. Introduction

The detector procurement and selection process for the WFC3 IR channel has recently delivered detectors with good QE, stability and noise properties. On this basis, we can now determine whether an instrument using these detectors would meet the original CEI spec requirements. To this purpose we have implemented a relatively simple tool that does not rely on the current version of the instrument ETC. This allows us treat different instruments (e.g. WFC3 and NICMOS) in the same way, and gives us the flexibility needed to quickly explore how various parameters affect the final instrument performance. It also provides an independent check to the estimates of the more sophisticated ETC package.

As part of the performance verification, we have also checked the thermal background of the instrument by using the most recent operating temperature estimates for the various components. This is documented in an accompanying ISR (Robberto & Stiavelli, 2003).

This ISR documents our performance calculations and results. The input parameters are given in Sect. 2. The main results are described in Sect 3 and discussed in Sect. 4.

2. Input parameters

2.1 Filters

We have focused our attention on the F110W (J) and F160W (H) broad-band filters and on the F126N narrow-band filter. The NICMOS detectors had a relatively high peak QE in the red and much lower QE at shorter wavelengths. F126N was chosen because it is a narrow-band filter at relatively short wavelengths, where the QE curves still show large differences between different detectors. A high QE in this region could produce a large sensitivity gain. Even though NICMOS does not have such a filter, we have assumed that it was available in our NICMOS simulation for the sake of comparison.

2.2 Sky brightness

Following WFC3 ISR 2002-02, we adopted as average sky background in the J and H band, respectively, 0.023 and 0.014 photons $\text{HSTarea}^{-1}\text{s}^{-1}\text{A}^{-1}\text{arcsec}^{-2}$. These background values were scaled into photons impinging on a pixel by adopting a pixel size of 0.128 arcsec for WFC3 (geometric average of the X and Y pixel sizes), 0.075 arcsec for NICMOS Camera 2, and 0.2 arcsec for NICMOS Camera 3. For F126N we adopt the same average sky background as for F110W.

2.3 Detector QE

We have computed the average QE over the filters, based on the best information available at this time. The adopted values are shown in Table 1 below.

	FPA64	CEI Req.	RSC Req.	CEI Goal	NIC-NCS	NIC noNCS
F110W	0.419	0.475	0.4	0.575	0.3	0.181
F160W	0.709	0.583	0.381	0.683	0.43	0.302
F126N	0.488	0.5	0.45	0.6	0.33	0.194

Table 1: Adopted QE values for the three filters.

2.4 Optics and filter throughput

We have assumed that the throughput of the OTA, including the cold stop, is 0.744 for both WFC3 and NICMOS. This is justified by the very similar cold stop design for both instruments, but it does not include the effect of the NICMOS cold stop misalignment. For NIC2, the misalignment reduces the throughput from 0.74 to 0.67 (Robberto et al. 2000).

Following Ball SER OPT-072, we adopt for WFC3 the optics throughputs of 0.857 and 0.911, respectively, for the J and H bands. The CEI Spec throughput was 0.72 and 0.73, respectively, in J and H. The F110W, F160W, and F126N filters have average transmission of 0.9582, 0.9425, and 0.8426, respectively, over the bandpass. We adopted bandpasses of 500 nm for F110W, 290 nm for F160W, and 17 nm for F126N.

For NICMOS we have adopted the throughput of 0.84, including the filter, for both J and H. The NICMOS filter bandpasses have been taken to be 600 nm for F110W, 400 nm for F160W, and 17 nm for the fictional F126N.

2.5 PSF sharpness

In order to be able to evaluate objectively the signal-to-noise ratio of a given exposure without going through the somewhat arbitrary process of defining extraction apertures, we have adopted the assumption of optimal extraction. Under this assumption the number of pixels contributing to the noise is given by the inverse of the PSF sharpness. Using simulated PSFs we have adopted for WFC3 the values of sharpness 0.1715, 0.122, and 0.153 for F110W, F160W, and F126N, respectively. The NIC2 sharpness values for the same filters are 0.074, 0.043, 0.074 and for NIC3 0.202, 0.204, and 0.202, respectively. For NICMOS the sharpness has been determined by using Tiny Tim's PSFs.

2.6 Detector noise parameters

The detector noise parameters are given in Table 2 below.

	FPA64	CEI Req	RSC Req	CEI Goal	NIC3-NCS	NIC3 pre NCS
d.c. (e/pixel/s)	0.1	0.2	0.4	0.1	0.1	0.15
Ron (e rms/pixel)	15.6	10	10	7	22	22

Table 2: adopted detector noise parameters.

For NIC2 we have adopted a read out noise RON=20 e rms/pixel instead of the current published value RON=22 e.

2.7 WFC3 internal background

We have recomputed the expected internal backgrounds for the instrument by using the most recent values for the temperature of the various components. Because of the importance of the red cutoff, our calculations are in photons convolved by a cutoff function. This function has a value of 1 at wavelengths shorter than the cutoff wavelength minus 50nm and goes linearly to zero at the cutoff wavelength plus 50 nm. The cutoff function has a value of 0.5 at the cutoff wavelength. This definition allows us to calculate very accurately the thermal background counts by simply multiplying the thermal background photons by the QE in the H band. The temperatures adopted are partly based Chris Miller's measurements of 10-18-02 at Ball and are summarized in Table 3.

Inner radiation shield	-88 C
Enclosure window	-32 C
Top of inner radiation shield	-80 C
Baffle	-33 C
Filter wheel	-29 C
Optical bench	5C
Pick-off	14.6 C
M1	15 C
M2	17 C

Table 3: temperatures of various WFC3 components.

The values of the thermal background have been found to be 0.08 ph/s/pixel in the F110W and F126N filters and 0.31 ph/s/pixel in F160W.

For NICMOS we have adopted 0.114 and 0.763 ph/s/pixel, respectively, for NIC2 and NIC3 in F160W. We have not included a thermal contribution for F110W and F126N.

2.8 Source count rates and exposure strategy.

We have considered faint targets, so that the required signal-to-noise would be reached in multi-orbit exposures. We have assumed that the detector would be read-out non-destructively with total readout noise reported in Section 2.6, and reset every 2400s. For the broad-band images we have considered a point source of AB mag = 28 in both J (27.2 in the Vega system) and H (26.6 in the Vega system). This corresponds to 22.91 nJy or $1.3 \cdot 10^{-4}$ and $9.78 \cdot 10^{-5}$ photons HST area⁻¹ s⁻¹ A⁻¹ in J and H, respectively. For the narrow band filter we have considered an AB mag =25 (J=24.2 in the Vega system) or 363.1 nJy. This translates into $2.07 \cdot 10^{-3}$ photons HST area⁻¹ s⁻¹ A⁻¹.

For the extended source calculations we have considered values of surface brightness of AB=26 mag arcsec⁻² and AB=23 mag arcsec⁻², respectively, for the broad and narrow band filters.

In all cases we have required a S/N=10 (either per source or per arcsec²).

3. Results

3.1 Point source speed

We focus on full orbit exposures since they are representative of a deep survey. The point source speed is defined as the inverse of the number of orbits needed to achieve a given signal to noise ratio (hereafter S/N) on a faint point source, i.e. a small number of orbits to achieve a given S/N implies a high speed. When normalized to a particular detector-optics configuration, the speed does not depend on the requested S/N and source magnitude, as long as they are such that one remains in a multi-orbit regime. We carried out our calculations requiring a S/N=10 and considering for the J and H calculations sources with AB=28 (22.91 nJy) and for the narrow band calculation a source with AB=25 (363.1 nJy).

The normalized point source speed results are given in Figure 1 and Table 4. Results are shown for: a) the as-built WFC3 with FPA64; b) the RSC spec detector; c) the CEI goal detector, all normalized to the CEI requirements. The as built instrument with FPA 64 beats in performance the instrument as described in the CEI requirements instrument. For comparison we also show the performance of NICMOS Camera 2 and 3 before and after the installation of the NCS. In terms of point source sensitivity, in the J band and in the narrow band filter the WFC3 with FPA64 performs better than NICMOS. In the H band WFC3 performs slightly better than NICMOS camera 3 before the installation of NCS but not as well as NICMOS Camera 3 with the NCS. This is due to the fact that the NICMOS H band filter is broader than that of WFC3, due to the shorter wavelength cutoff of the WFC3 IR detectors.

	FPA64	RSC Req	CEI Goal	NIC3NCS	NIC2NCS	NIC3	NIC2
F110W	1.13	0.62	1.49	0.54	0.60	0.30	0.31
F160W	1.97	0.39	1.50	2.21	1.34	1.91	0.96
F126N	1.53	0.50	2.22	0.85	0.38	0.36	0.16

Table 4: Normalized point source speed for the as-built WFC3 with FPA64, for the RSC req detector and the CEI Goal detector, all normalized to that of the instrument described in the CEI requirement. Also shown is the performance of NICMOS camera 2 and 3 before and after the installation of the NCS.

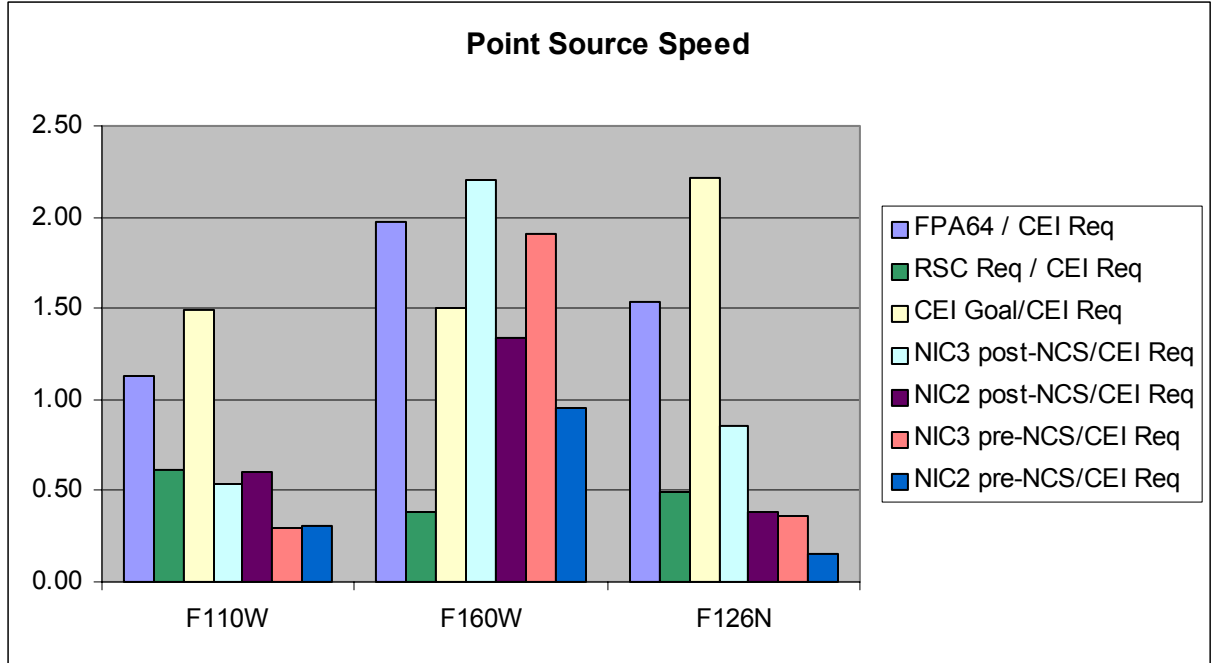


Figure 1: comparison of the normalized point source speed for WFC3 with the various requirements and NICMOS.

3.2 Extended source speed

We have also considered the speed of achieving a given S/N for an extended source. The S/N is computed over 1 square arcsec. The main results are shown in Table 5 and Figure 2. WFC3 with FPA 64 still outperforms the CEI requirement instrument, NICMOS camera 2 and NICMOS camera 3 before the NCS. NICMOS camera 3 with the NCS outperforms WFC3 IR for extended sources, mostly due to the large pixel size.

	FPA64	RSC Req	CEI Goal	NIC3NCS	NIC2NCS	NIC3	NIC2
F110W	1.13	0.61	1.49	1.93	0.30	0.99	0.16
F160W	1.88	0.42	1.43	2.57	0.52	1.68	0.35
F126N	1.54	0.49	2.24	1.62	0.26	0.67	0.11

Table 5: Extended source speed for the as-built WFC3 with FPA64, for the RSC requirement detector and the CEI Goal detector. The normalization speed is that of the instrument as described in the CEI requirement. Also shown is the performance of NICMOS camera 2 and 3 before and after the installation of the NCS.

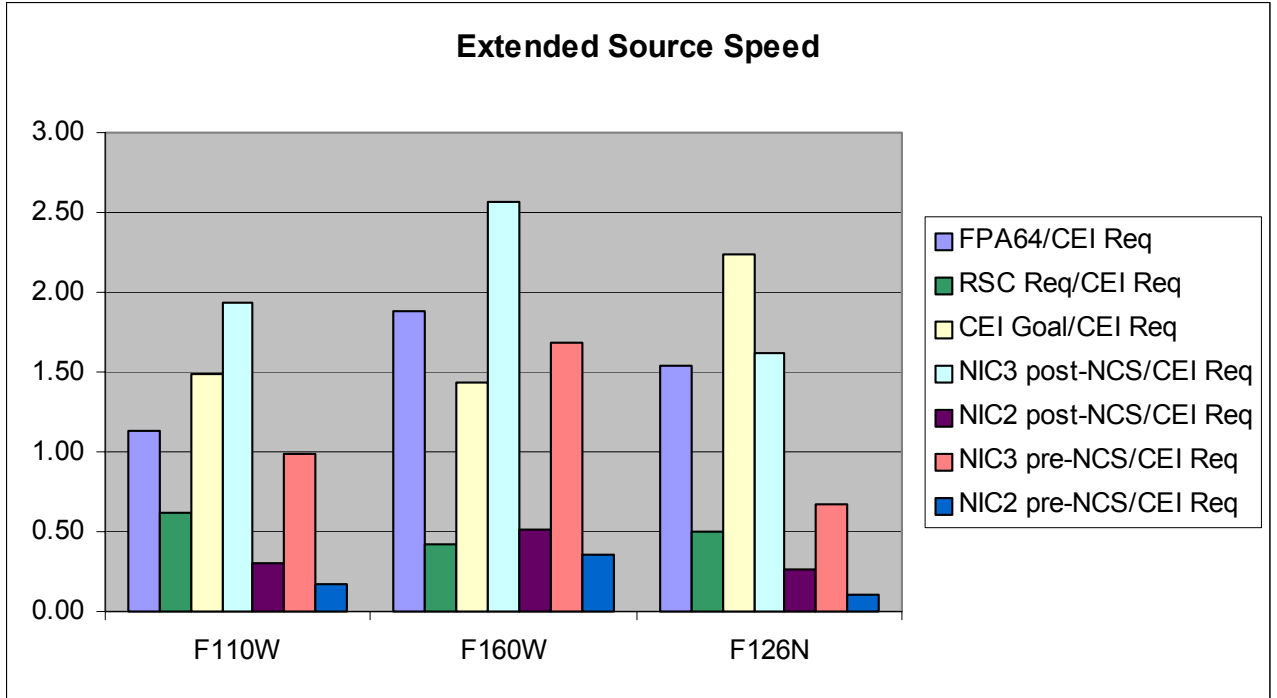


Figure 2: comparison of the normalized extended source speed for WFC3 with the various requirements and NICMOS.

3.3 Discovery Efficiency

Pure speed considerations do not take into account the larger field of view of WFC3. The combination of a large field of view with smaller pixels is the main strength of WFC3 IR over NICMOS-Camera 3. Whereas the increase in photometric accuracy associated to the smaller pixel size cannot be easily factorized into a single parameter, the effect of both sensitivity and field of view can be measured defining the Discovery Efficiency, as the product of the FOV times the point source speed. The Discovery Efficiency provides a direct estimate of the time needed to carry out a wide-area deep survey. The values of discovery efficiency are given in Table 6 and Figure 3. The results are normalized to the WFC3 CEIs requirement. It is clear that the discovery efficiency of WFC3 with FPA64 exceeds that of the CEI requirements instrument and, by a large factor, that of NICMOS.

	FPA64	RSC Req	CEI Goal	NIC3NCS	NIC3
F110W	1.13	0.62	1.49	0.08	0.05
F160W	1.97	0.39	1.50	0.34	0.29
F126N	1.53	0.50	2.22	0.13	0.05

Table 6: Discovery Efficiency for the as built instrument with FPA64, for the RSC req. detector and the CEI Goal detector. The normalization discovery efficiency is that of the instrument as described in the CEI requirements. We also show the performance of NICMOS camera 3 before and after the installation of the NCS. We are omitting NICMOS Camera 2 since its small field of view would lead to a very small discovery efficiency.

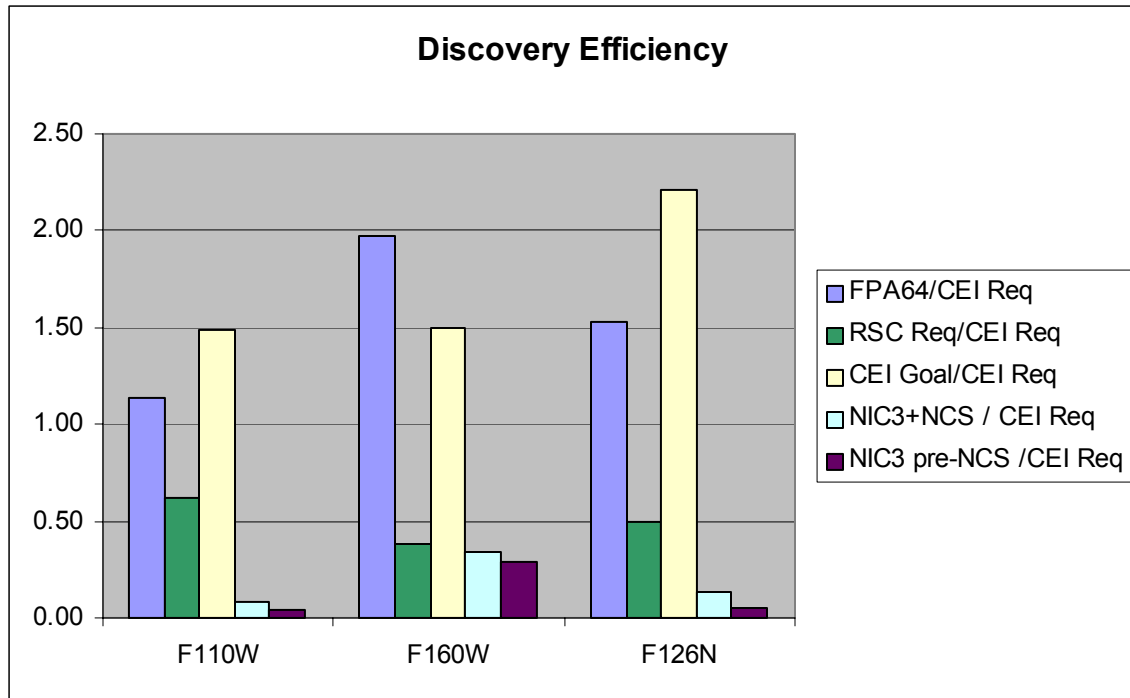


Figure 3: comparison of the discovery efficiency for WFC3 with the various requirements and NICMOS.

3.4 Delta performance

We expect that a number of detectors will be available for selection of the flight and flight spare FPAs. In view of the selection process, it is important to evaluate how changes in the dark current, readout noise, and sensitivity characteristics affect the final instrument performance. In Table 7 and Figure 4 we show how the point source speed is improved by varying these instruments parameters by amount possibly within reach if feature lots are produced. We have considered a reduction of dark current by a factor two, a reduction of the readout noise to 10 electrons per pixel rms, and an improvement in the QE (up to 60 per cent in J and 80 per cent in H) to the level of the best Lot 6 parts, characterized by much higher readout noise and instability. High QE would clearly provides the most significant gain.

	FPA64	DC 0.05	RON 10e	Extra QE
F110W	1.13	1.21	1.23	1.77
F160W	1.97	2.11	2.14	2.29
F126N	1.53	1.88	1.97	2.19

Table 7 : improvements in point source speed by changing detector parameters. Any improvement would affect significantly the narrow band speed, but only improvements in QE would significantly affect the speed in the broad band filters.

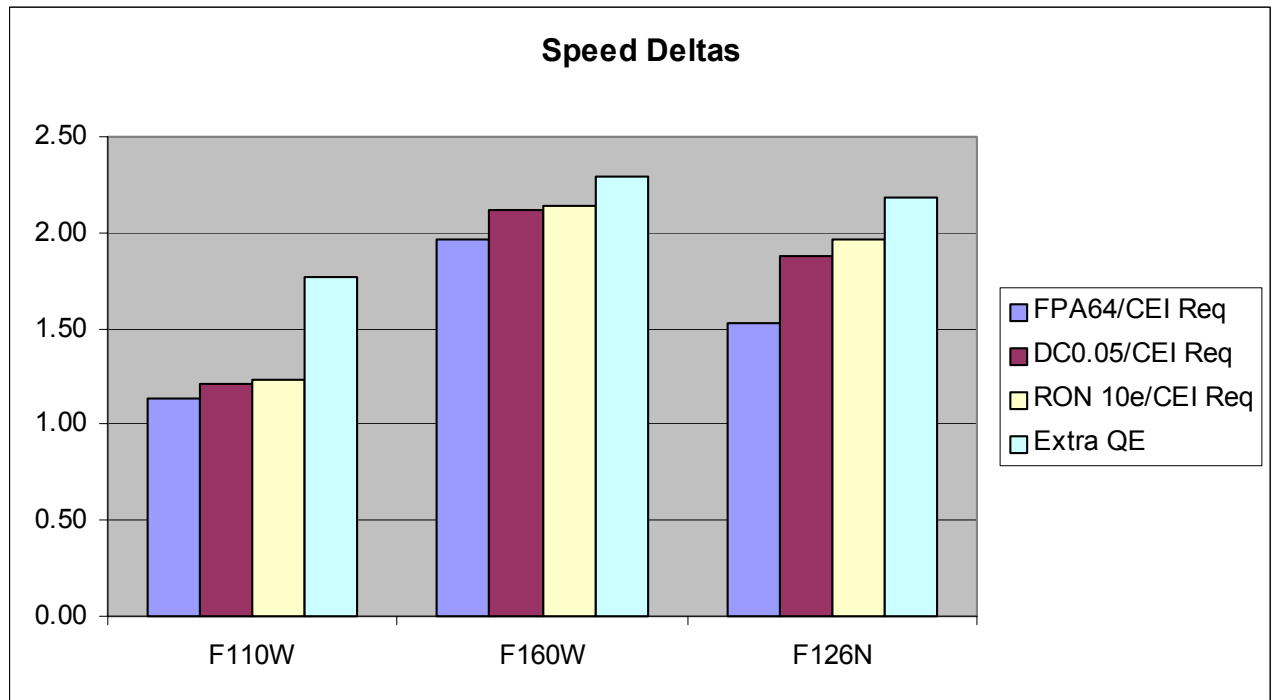


Figure 4 : improvements in the point source speed obtained by improving the dark current, readout noise or quantum efficiency.

4 Discussion and conclusions

The WFC3 IR channel with as built optics and available detectors has a performance superior to that of the instrument as described in the CEI requirements in any of the metrics considered above. In addition, WFC3 IR will have a discovery efficiency significantly higher than that of NICMOS in both J and H bands. This is shown in the table 8 where the values of discovery efficiency are given normalized to NICMOS camera 3 before the installation of NCS. In the combined J plus H metric, corresponding to a two band wide area, deep, survey WFC3 with FPA64 exceeds the discovery efficiency of NICMOS before and after the installation of NCS by a factor of 15 and 10, respectively.

	FPA64	CEI Req	RSC Req	CEI Goal	NIC3	NIC3_old
F110W	25.05	22.12	13.61	32.88	1.83	1.00
F160W	6.75	3.43	1.33	5.15	1.15	1.00
F126N	28.13	18.35	9.13	40.66	2.39	1.00
JH	15.90	12.77	7.47	19.01	1.49	1.00

Table 8 : Discovery Efficiency for the as built instrument with FPA64, for the CEI req instruments, for the RSC req. detector and the CEI Goal detector. The normalization discovery efficiency is that of the pre-NCS NICMOS camera 3. We also show the performance of

NICMOS camera 3 after the installation of the NCS, and the discovery efficiency for a deep, wide-field survey made with a combination of J and H filters.

REFERENCES

Robberto et al. 2000. Proc. SPIE , 4013, 386

Acknowledgements

We thank Neill Reid for review the manuscript and Daniela Calzetti for a critical review of the various parameters and, especially, of the comparison with NICMOS.